Engineered Science
DOI: https://dx.doi.org/10.30919/es1200

Anti-swelling Zwitterionic Nanocomposite Hydrogels with Biocompatibility as Flexible Sensor for Underwater Application

Zhicheng Jiang,[1,2] Ruicheng Sha,[1] Yunbo He,[1] Mengshuang Wang,[1] Wenjing Ma,[3] Shuting Gao,[2] Mengni Zhu,[1] Yue Li,[1] Mengying Ni[1] and Min Xu[1,*]

Abstract

The increase in underwater activities has driven the demand for underwater flexible sensors, which can detect various signals from both humans and the environment in real time to improve work efficiency and ensure safety. However, the fabrication of underwater sensors remains challenging due to the swelling of hydrogels in water and the non-eco-friendliness of the sensors, which poses significant risks to users and the application environment. Here, a hydrogel-based sensor composed of poly [2-(methacryloyloxy) ethyl] dimethyl-(3-sulfopropyl) ammonium hydroxide and bacterial cellulose nanofibers, featuring self-adhesion, biocompatibility, and anti-swelling behavior, is fabricated using an environmentally friendly method. The electrostatic interaction between zwitterionic functional groups (positively charged -R_3N^+ groups and negatively charged -SO^{3-} groups) endows the hydrogel with excellent anti-swelling behavior in aquatic environment. Owing to these characteristics, the hydrogel sensor is capable of monitoring movements in both air and underwater environment. Based on the hydrogel sensor, an intelligent communication system is developed to facilitate information transmission in water. Moreover, the excellent biocompatibility of the hydrogel sensor highlights its safety for users and the environment, demonstrating its great promise for electronic skin. As such, the biocompatible hydrogel sensor with anti-swelling capabilities provides a promising route to promote the development of wearable devices.

Keywords: Hydrogel sensor, Biocompatibility; Anti-swelling; Eco-friendly; Underwater.
Received: 21 September 2023; Revised: 02 December 2023; Accepted: 04 December 2023.
Article type: Research article.

1. Introduction

With the rapid development of the Internet of Things (IoT), wearable sensors acting as core components are gaining increasing research interest research interest due to its capacity to convert external stimuli such as temperature,[1-3] pressure,[4,5] strain,[6] humidity[7,8] wearable sensors acting as core components are gaining increasing research interest research interest due to its capacity to convert external stimuli,[11,12] intelligent robots,[13] human-machine interfaces,[14] *etc*. As candidate materials for wearable sensors, conductive hydrogels have been widely reported due to their outstanding flexibility, deformability, stretchability, and biotissue-like moduli.[15,16] However, further technological advancements impose higher requirements on wearable hydrogel sensors for extreme application environments, particularly underwater. Nowadays, an increasing number of human activities are taking place underwater, such as underwater detection, underwater rescue, fish kinematics research, and more. To ensure the safety and improve the work efficiency of underwater activities, it is both significant and urgent to design wearable hydrogel sensors that can be utilized in underwater applications.

However, up to now, it remains a significant challenge to realize the underwater application of hydrogel sensors because traditional hydrogels suffer from remarkable swelling in water, leading to compromised mechanical and sensing properties. Recently, a considerable amount of research has been reported on designing wearable hydrogel sensor applications in water, such as solvent-exchange,[17] hydrophobic aggregation,[18-20]

[1] *School of Physics and Electronic Science, East China Normal University, Shanghai 200241, China.*
[2] *Jiangxi Chenguang New Materials Co., Ltd, Jiujiang 332500, China.*
[3] *Joint Laboratory of Advanced Biomedical Materials (NFU-UGent), Jiangsu CoInnovation Center of Efficient Processing and Utilization of Forest Resources, Nanjing Forestry University, Nanjing 210037, China.*
**Email:* xumin@phy.ecnu.edu.cn (M. Xu)

electrostatic interaction,[21] and high-crosslinking densities.[22] These strategies can successfully inhibit the swelling behavior of the hydrogel sensors in water, which was vital for improving the applicability of sensors used in aquatic environments. Unfortunately, some of these strategies used non-eco-friendly reagent such as dimethyl sulfoxide (DMSO) and hydrochloric acid (HCl), which pose a risk of leakage during use and may cause potential threats to users, including skin inflammation, allergies or unpredictable pollution to the environment. Another method to achieve anti-swelling capacity of hydrogel sensors was to use high-crosslinking densities. However, this strategy inevitably leads to a high Young's modulus, which reduces the flexibility of the hydrogel sensor and decreases the sensing performance and wearing comfort of the wearable sensor. Therefore, it is crucial yet challenging to develop an anti-swelling hydrogel sensor with good biocompatibility and environmentally friendly properties for wearable underwater applications using an eco-friendly method.

As a kind of zwitterionic polymer, poly [2-(methacryloyloxy) ethyl] dimethyl-(3-sulfopropyl) ammonium hydroxide (PSBMA) contains both positively charged $-R_3N^+$ groups and negatively charged $-SO_3^-$ groups.[21] Recently, PSBMA has attracted extensive research interests in the fields of gel electrolytes,[23,24] antifouling materials,[25] and biomedical materials[26] owing to its high hydrophilicity, high ion density, and excellent biocompatibility.[27] PSBMA exhibits strong electrostatic interactions due to the high-density ions, which would promote to form self-association, and water molecules can be eliminated, providing the possibility for the preparation of anti-swelling hydrogels.[21] Unfortunately, PSBMA is difficult to construct hydrogel sensors due to its poor mechanical properties, so that there have been rarely exploration on hydrogel sensor for underwater application based on PSBMA so far.

Herein, we innovatively designed an anti-swelling hydrogel with excellent biocompatibility and self-adhesion performance using an eco-friendly method. The hydrogel network consists of bacterial cellulose nanofibers (BCN) and PSBMA. To ensure the eco-friendliness of the preparation process and the compatibility of hydrogel, poly (ethylene glycol) diacrylate (PEGDA), a non-toxic cross-linking agent, was chosen to facilitate the formation of the PSBMA network structure. In addition, biocompatible BCN was used as a mechanical reinforcement material to enhance the mechanical properties of hydrogel based on hydrogen bonds. PSBMA contains abundant negatively charged $-SO_3^-$ groups and positively charged $-R_3N^+$ groups, which form strong electrostatic interactions and inhibit the diffusion of water into the gel, giving the hydrogel excellent anti-swelling properties. Furthermore, due to the charged functional groups of PSBMA, the hydrogel exhibits extensive adhesion behavior. The PSBMA-BCN hydrogel can be assembled into an anti-swelling, self-adhesive wearable sensor with outstanding sensitivity for monitoring both large-scale and subtle deformation. To provide proof-of-concept for its potential applications, the PSBMA-BCN hydrogel sensor was developed for underwater uses, including communication and motion detection. Importantly, cytocompatibility results demonstrated the PSBMA-BCN hydrogel's safety, highlighting its great potential to serve as the basis for the next generation of green hydrogel-based sensors for water applications.

2. Experimental section

2.1 Materials

Bacterial cellulose (BC) hydrogels were applied by Hainan Guangyu Biotechnology Co., Ltd (Hai nan, China). [2-(methacryloyloxy) ethyl] dimethyl-(3-sulfopropyl) ammonium hydroxide (SBMA, 99%) and Polyethylene glycol diacrylate (PEGDA) were purchased from Sigma-Aldrich. Ammonium persulfate (APS), sodium hydroxide (NaOH), and hydrochloric acid (HCl) were purchased form Sinopharm Chemical Reagent Co., Ltd. Cell culture materials including Dulbecco's modified Eagle medium (DMEM), fetal bovine serum (FBS), trypsin, and phosphate buffered saline (PBS) were purchased from Thermo Fisher Scientific.

2.2 Preparation of BCN dispersions

The BCN dispersions was prepared via a simple method previously reported by Li group.[28] Briefly, the BC hydrogels were washed with 1 M NaOH solution for removing the culture medium and bacterium, followed by repeatedly washing with deionized water to neutrality. Then, BC hydrogels were cut into small pieces and dispersed in deionized water. Subsequently the obtained BC pieces were pulped with a mechanical homogenizer to obtain a uniform BCN dispersion (2mg mL^{-1}) at the speed of 10000 r min^{-1} for 30 min.

2.3 Preparation of hydrogel

The PSBMA-BCN hydrogel was prepared by an eco-friendly method. First, the BCN dispersion (2mg mL^{-1}) was mixed with deionized water and stirred for 2 h to form a uniformly dispersed solution. Subsequently, 1.5 g SBMA and 12 μL PEGDA were added and mixed evenly. Afterwards, 120 μL (0.1 g mL^{-1}) APS was added to the above solution and stirred for 10 min to obtain the homogeneous precursor solution.

Finally, the precursor solution was transferred into reaction mold. And the hydrogel was formed by polymerization at 60 ℃ for 6 h. The hydrogel was defined as PSBMA-BCN-x, where x means the contents of BCN. The detailed information was showed in Table S1.

2.4 Characterization

The chemical structure was analyzed by the Fourier transform infrared (FT-IR) spectrometer (Nicolet-Nexus 670 spectrophotometer) and XPS spectrometer (Escalab 250Xi). The micro-morphology of hydrogel and BCN were determined by scanning electron microscopy (SEM) (Hitachi S-4800 FE-SEM). The transmittance of the hydrogel sample was evaluated by UV-2700 form SHIMADZU.

2.5 Mechanical performance

The universal mechanical properties were measured using a tensile machine (INSTRON 5943) at room temperature. For tensile tests, the hydrogel samples were cut into a cylindrical shape (4.5 mm diameter, 50 mm length) at a tensile speed of 50 mm min^{-1}. Toughness was calculated by integral area of the stress-strain curve. For compression tests, the samples were cut into a cylindrical shape (20 mm in diameter, 10 mm in height) under compression speed of 10 mm min^{-1}. The toughness was calculated by integral area of the stress-strain curve.

2.6 Self-Adhesion performance

Adhesion property of hydrogels were measured by a tensile machine (INSTRON 5943). The samples cut into pieces 20 mm (length) × 20 mm (width) × 2 mm (thickness) were sandwiched by two pieces of substrates including Ti tapes, PTFE, glass, and porcine skin, respectively. Before testing, the samples were required to be continuously pressurized for 5 min. The test velocity was 20 mm min^{-1} under room temperature.

2.7 Swelling behavior

The swelling behavior was evaluated by soaking hydrogel in various solvents at room temperature and weighting the hydrogel samples. The swelling ratio (SR) is defined as follows:[17]

$$Swelling\ ratio = \frac{W_t - W_0}{W_0} \times 100\% \quad (1)$$

where W_t is the weight of the swollen hydrogel and W_0 is the weight of original hydrogel.

2.8 Electrical measurement

The real-time resistance signal changes of the hydrogel sensors were monitored by using Tonghui TH2830 (Changzhou, China). The relative resistance changes (RRCs) of the hydrogel can be calculated by the equation:[29]

$$\frac{\Delta R}{R_0} = \frac{R - R_0}{R_0} \times 100\% \quad (2)$$

where R_0 and R are the original and real-time resistance of hydrogel sensors, respectively.

The gauge factor (GF) is defined as:

$$GF = \frac{\frac{\Delta R}{R_0}}{\varepsilon} \quad (3)$$

where ε is the applied strain.[29]

2.9 Biocompatibility evaluation

The biocompatibility of PSBMA-BCN hydrogel was assessed by using Cell Counting Kit-8 (CCK-8) assay. PSBMA-BCN hydrogels were soaking in culture medium for extraction at 37 ℃ for 12 h. Human amniotic epithelial cells (HAECs) (5000 cells/well) were seeded in 96-well cell culture plates with different extraction. After incubation for 24 and 48 h (37 ℃, 5% CO_2), the staining reagents (CCK-8) were incubated with cells for 30 min. The blank control group and positive control group were culture medium and PBS buffer, respectively. Then, the optical density (OD) corresponding to the number of live cells was immediately measured using a spectrophotometer (Spectra Max iD5) at 450 nm. The cell viability was calculated by the following equation.[3]

$$Cell\ viability = \frac{A_{sample}}{A_{control}} \times 100\% \quad (4)$$

where A_{sample} is the absorption of experimental group, and $A_{control}$ refers to the absorption of the untreated group.

To further observe the cells, the blank control groups and experimental group were stained using a Live/Dead Viability/Cytotoxicity Kit (Beyotime Biotechnology). After incubation for 24 and 48 h, the cells were washed with PBS. Subsequently, the stain was added to the cells and incubated for additional 30 min. Finally, the stained cells were observed using a florescent microscope (DMI8, Leica).

3. Results and discussion

3.1 Preparation hydrogel

An anti-swelling and biocompatible hydrogel, comprising bacterial cellulose nanofibers (BCN) and PSBMA, was fabricated using an eco-friendly method. As illustrated in Scheme 1a, the SBMA monomer was added to the BCN dispersions to form a homogeneous mixture. Subsequently, the polymerization of SBMA was initiated by APS and cross-linked by PEGDA to finally obtain the PSBMA-BCN hydrogel. The BCN exhibited a large aspect ratio, which allows for the formation of continuous entanglements within

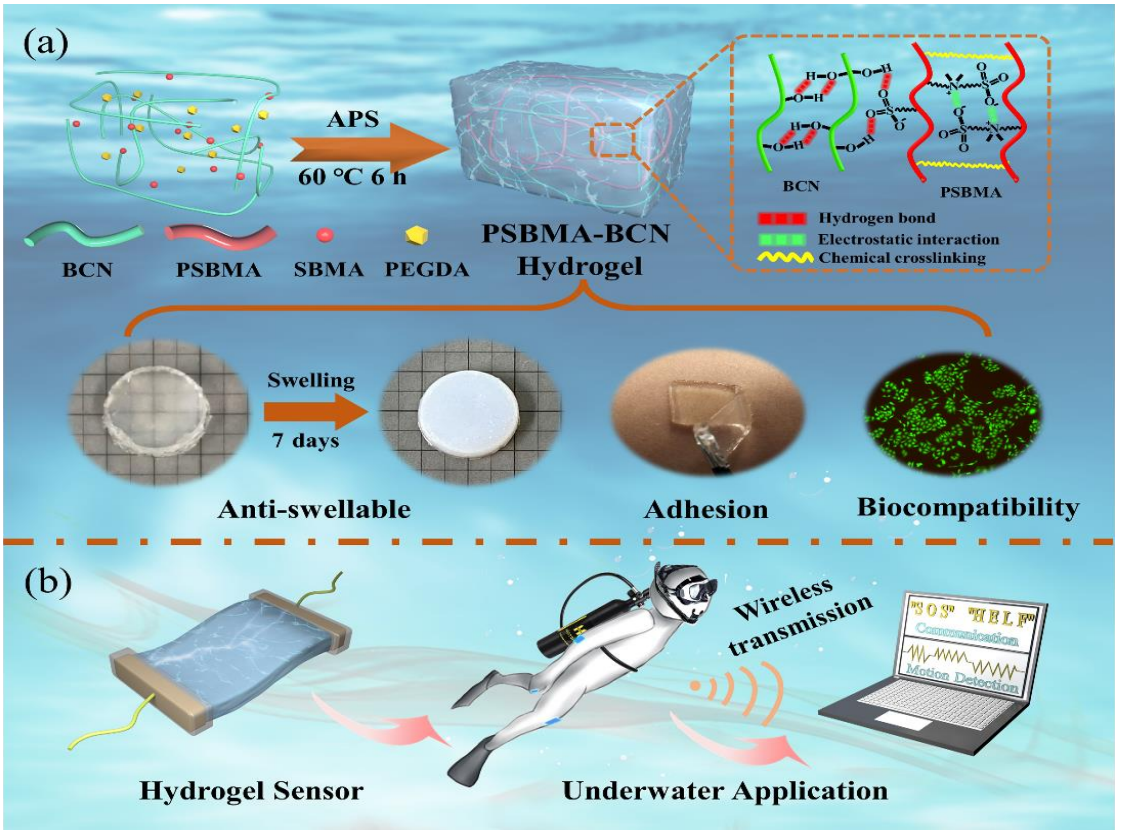

Scheme 1. (a) Schematic structure of PSBMA-BCN hydrogel and its properties. (b) PSBMA-BCN hydrogel sensor for underwater applications.

the PSBMA network. Additionally, the hydroxyl groups of the bacterial cellulose nanofibers can form hydrogen bonds with PSBMA. Therefore, the mechanical properties of the PSBMA-BCN hydrogel have been improved. Notably, the negatively charged $-SO_3^-$ groups and positively charged $-R_3N^+$ groups in PSBMA endow the hydrogel with widely applicable adhesion properties. In addition, the strong electrostatic interaction between the positively charged $-R_3N^+$ groups and the negatively charged $-SO_3^-$ groups facilitated charge association within the PSBMA-based hydrogel, endowing it with excellent anti-swelling properties. Importantly, there were no organic solvents in the system; thus, the prepared hydrogel exhibits excellent environmental friendliness and biocompatibility, which enables a wider range of potential applications in the fields of flexible sensors, electronic skin, and more. Due to its excellent anti-swelling properties, the hydrogel demonstrates significant potential as a wearable sensor in underwater applications, such as underwater communication and motion detection (Scheme 1b).

3.2 Characterization of hydrogel

The structure of the hydrogel was investigated using Fourier-transform infrared (FT-IR) spectroscopy and X-ray photoelectron spectroscopy (XPS). In the FT-IR spectra of the PSBMA-BCN hydrogel (Fig. S1), the strong absorption peak at 1490 cm^{-1} was attributed to C-N=. The two absorption peaks at 1182 cm^{-1} and 1037 cm^{-1} were attributed to the symmetrical and asymmetric stretching vibrations of S=O, respectively. The characteristic absorption peak at 930 cm^{-1} was attributed to the stretching vibration of S-O. Neither the PSBMA nor the PSBMA-BCN samples exhibited a strong absorption peak at 1307 cm^{-1}, which corresponded to C-N^+, due to the electrostatic influence of N^+ on SO_3^-. In addition, the FT-IR spectra of SBMA and PSBMA hydrogels exhibited a strong characteristic absorption peak at 3459 cm^{-1}, which was ascribed to -OH groups generated from moisture absorbed from the air, induced by the strong water absorption of zwitterionic functional groups. However, in the spectrum of the PSBMA-BCN hydrogel, the characteristic peak of -OH shifted to a higher frequency (3434 cm^{-1}), indicating the formation of hydrogen bonds between bacterial cellulose nanofibers and PSBMA.[21,30,31] Furthermore, the chemical structure was analyzed using XPS spectroscopy. The analysis of the XPS spectra is presented in Fig. S2.

BCN exhibits hydrophilicity due to its abundant hydroxyl groups, which endows it with excellent dispersion in water. As shown in Fig. S3a, the BCN dispersion in the glass bottle remained uniform and did not aggregate or precipitate after 30 days. The SEM image confirmed that BCN exhibited a fibrous

structure with a high aspect ratio, which could form chain entanglements in the hydrogel, thereby enhancing the mechanical properties of PSBMA. Fig. S3b illustrates the micromorphology of the PSBMA hydrogel, which features an abundant three-dimensional smooth pore structure. After the introduction of BCN, the micromorphology of the hydrogel exhibited a wrinkled structure, with BCN being more embedded in the polymer, indicating high compatibility between BCN and PSBMA (Figs. S3c-d).

3.3 Mechanical properties

The mechanical properties of the PSBMA-BCN hydrogel were characterized (Fig. 1). As illustrated in Fig. 1a, the PSBMA-BCN hydrogel exhibited excellent flexibility, allowing it to be stretched and knotted without any fractures. Furthermore, a small piece of hydrogel (4.5 mm in diameter and 60 mm in length) demonstrated the ability to lift a weight of 50 g. In addition, the hydrogel was sufficiently strong to resist compression and could quickly return to its original state after the pressure was removed. These results indicate the favorable mechanical properties of the hydrogel.

The mechanical properties of the hydrogel were quantitatively evaluated using a tensile tester. As a nanocomposite hydrogel, the properties of the PSBMA-BCN hydrogel can be enhanced by controlling the BCN content. Fig. 1b shows the stress-strain curves of nanocomposite hydrogels with different BCN contents. The tensile stress and elongation at break of the pure PSBMA hydrogel were both low. After the addition of BCN, the mechanical properties of the nanocomposite hydrogel were gradually improved. As the BCN content increased from 0% to 0.2%, the elongation at break increased from 328% to 520%, while the tensile stress increased from 2.7 KPa to 12.6 KPa. However, the elongation at break of the hydrogel did not improve with a further increase in BCN content, which may be due to the increased interaction between the BCN and PSBMA chains, hindering the movement of the molecular chains.[32] As shown in Fig. 1c, with the increase in BCN content, the toughness of the hydrogels initially increased and then declined, while the Young's modulus continued to increase. The PSBMA-BCN-

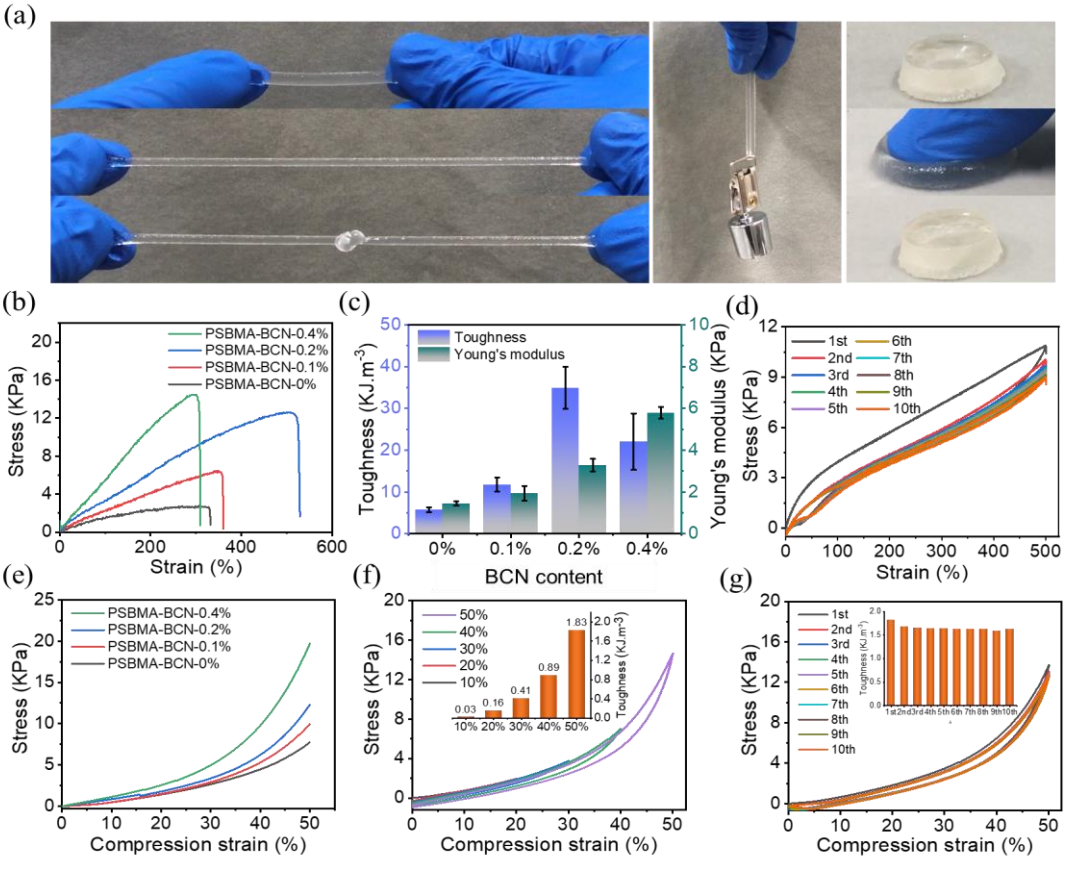

Fig. 1 Mechanical properties of the hydrogel. (a) Images of the PSBMA-BCN-0.2% hydrogel under stretching, knotting, weight lifting, and compression. (b) The stress-strain curves and (c) toughness and Young's modulus of the hydrogel with different BCN contents. (d) The repeated compression curves of the PSBMA-BCN-0.2% hydrogel. (e) The compression curves of the hydrogel with different BCN contents. (f) The compression curves of the PSBMA-BCN-0.2% hydrogel at different strains. Inset: The toughness of compression at different strains. (g) The repeated compression curves of the PSBMA-BCN-0.2% hydrogel. Inset: The toughness of compression at different times.

0.2% hydrogel exhibited the highest toughness (34.9 KJ m^{-3}) compared to the other hydrogels. These results also demonstrate the strong interaction between the BCN and PSBMA. In addition, the energy dissipation capacity of the nanocomposite hydrogel was investigated using a loading-unloading test (Fig. 1d). During the first stretching cycle, the hydrogel displayed a significant hysteresis loop. In the subsequent nine loading-unloading cycles, the stress-strain curves of the hydrogel depicted a negligible hysteresis loop and stress drop, indicating that the nanocomposite hydrogel has excellent self-recovery properties under stretching.

Additionally, the compression performance was also explored. The compression strength of nanocomposite hydrogel gradually increased with the increasing BCN contents (Fig. 1e). The cyclic loading-unloading compression curves at different strain were displayed in Fig. 1f**.** The compressive toughness gradually increased with the compressive strain increasing, and the compressive toughness of hydrogel reached 1.83 KJ m^{-3} under the compressive strain of 50%. Similarly, during the cyclic load-unload compressive cycle test, the hydrogel also exhibited excellent fatigue compression resistance, with constant hysteresis and toughness (Fig. 1g). These phenomena suggested that the composite hydrogel had superior mechanical recovery and energy dissipation ability based on the hydrogen bond between bacterial cellulose and polymer, and the electrostatic interaction among PSBMA chains. Due to their desirable mechanical performance, the PSBMA-BCN-0.2% hydrogels were used in following research.

3.4 Anti-swelling properties

In a liquid environment, conventional hydrogels easily swell, leading to inevitable solvent erosion and ultimately structural failure. Therefore, anti-swelling performance is vital for hydrogels in liquid environment applications. After 7 days of swelling, the nanocomposite hydrogel clearly demonstrated the restricted swelling performance of PSBMA-BCN hydrogels in both neutral water and acidic solution environments (Fig. 2a). Furthermore, the hydrogel changed from a transparent to an opaque state in both water and acidic solutions, which can be attributed to the strong electrostatic interactions within the networks, resulting in the association of intra- and inter-chains of PSBMA and microscopic phase separation.[33] After immersion in water, the pore structure of the hydrogel became denser, resisting the ingress of external water, which also demonstrated the strong electrostatic interactions between the polymer chains (Fig. 2b). As shown in Fig. 2c, the swelling kinetics of these hydrogels were determined by recording the weight changes. In water and an acidic environment (pH = 3), the swelling ratios of the hydrogels were ~11% and ~10% after soaking for 7 days, respectively. In contrast, the hydrogels swelled in an alkaline liquid (pH = 10), and the swelling ratio reached 144%. The mechanical properties of the PSBMA-BCN hydrogel were measured after soaking for 7 days in water, as depicted in Fig. 2d and Fig. S4a. After soaking in water and an acidic solution (pH = 3) for 7 days, the breaking strength and elongation at break of the hydrogel increased compared to the original hydrogel. This also indicates that the density of physical cross-linking points in the hydrogel increased after immersion in water, leading to a denser network structure. This assumption can also be confirmed by the SEM image of the hydrogel after soaking in water. However, due to the swelling behavior of the hydrogel in alkaline solution, the mechanical properties of the hydrogel immersed in an alkaline liquid (pH = 10) deteriorated after 7 days. The tensile strength and elongation at break were only 1.6 KPa and 123%, respectively. Fig. 2e and Fig. S4b show the adhesion properties of the soaked hydrogels adhered to glass. The adhesion strengths of the hydrogels after immersion in water and acidic solutions were 2.6 KPa and 2.1 KPa, respectively, which were better than those of the untreated gels. This can be explained by the increased cohesion of the hydrogels after soaking in water and an acidic solution.

The hydrogel contained abundant zwitterionic functional groups, including positively charged $-R_3N^+$ and negatively charged $-SO_3^-$. In a neutral solution environment, the electrostatic interactions between the positive and negative groups promote self-association, allowing water molecules to be eliminated and ensuring that the swelling behavior of the gel is restricted (Fig. 2f). In a low pH solution, $-SO_3^-$ groups are protonated, and the hydrogel behaves more like a polycation. However, the introduction of basic ions induces an electrostatic shielding effect, thus destroying the physical cross-linking points of the gel and leading to a greater swelling ratio.[34]

3.5 Self-adhesion properties

The adhesion behavior is an exceptionally favorable characteristic of the hydrogel-based sensor. Its adhesion ability enables the sensor to be firmly attached to the skin or other substrates, which is crucial for the functionality and reliability of wearable hydrogel electronic products, ensuring better interface communication. Given the abundant zwitterionic groups ($-SO_3^-$ and $-R_3N^+$) in PSBMA, the nanocomposite hydrogel can adhere to the surfaces of various substrates (such as polymers, metals, skin, and glass) through noncovalent interactions. The adhesion properties of the

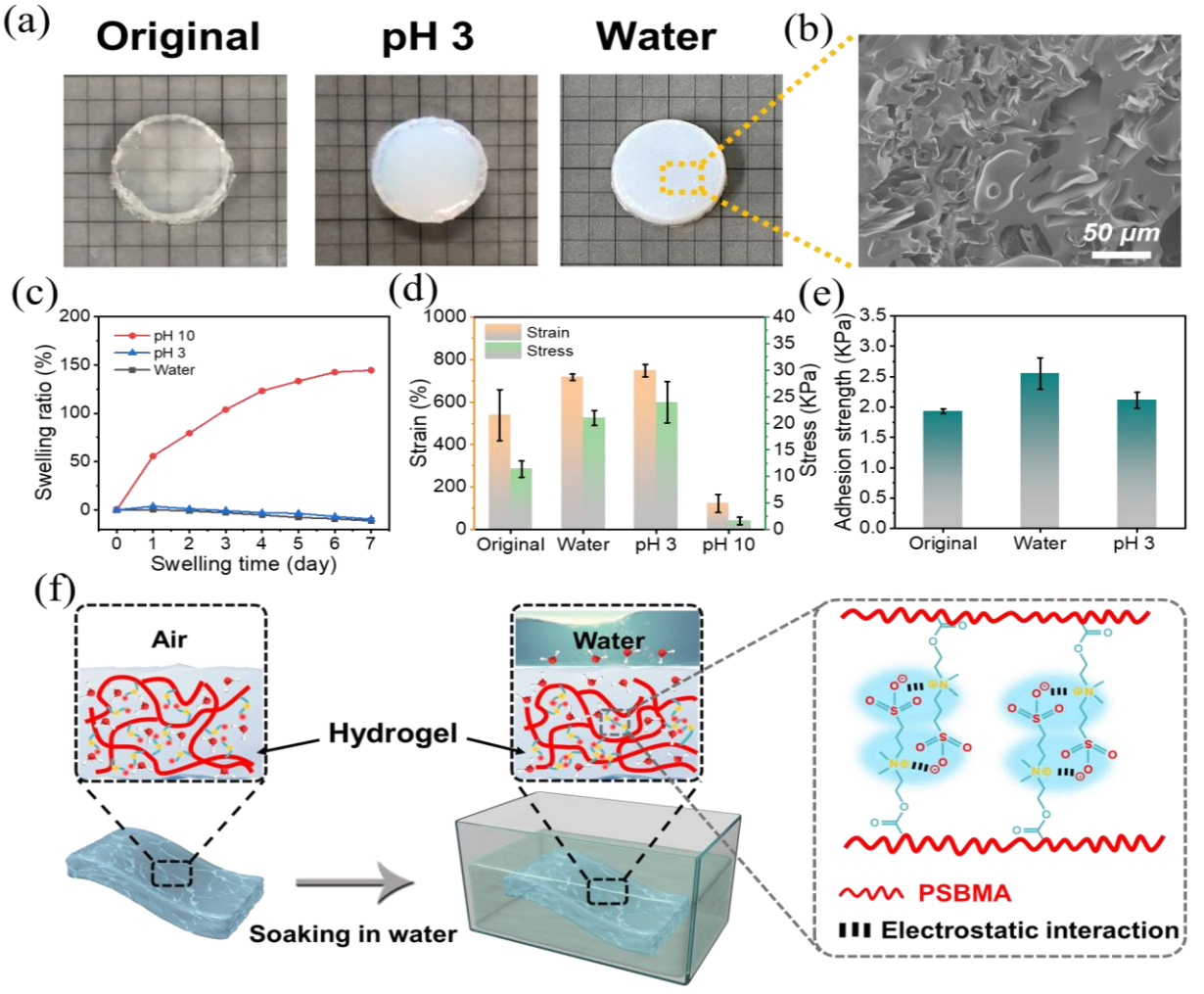

Fig. 2 Swelling behaviors of the hydrogel. (a) Swelling behavior of the hydrogels after 7 days in different liquid environment. (b) SEM image of the PSBMA-BCN hydrogel after soaking in water for 7 days. (c) Swelling ratio of the hydrogels as a function of swelling time. (d) Mechanical properties and (e) adhesion properties of the hydrogels after soaking in water for 7 days. (f) Schematic diagram of the anti-swelling mechanism of the PSBMA-BCN hydrogel.

hydrogel were evaluated using the lap shear test measurement (Fig. 3a). As shown in Fig. 3b and Fig. S5, the results indicated that the adhesion strengths were 0.7 KPa for PTFE, 1.9 KPa for glass, 1.8 KPa for Ti, and 1.1 KPa for porcine skin, respectively. The hydrogels also exhibited highly repeatable adhesiveness (Fig. 3c). Visually, the nanocomposite hydrogel can also adhere to other organic/inorganic surfaces and easily support their weight while retaining its position without detachment (Fig. 3d). Referring to the reported literature, we speculated that the strong adhesion on various substrates was due to the functional groups $-SO_3^-$ and $-R_3N^+$ that exhibited strong interactions, including hydrogen bonding, ion-dipole interactions, electrostatic attraction, metal coordination, and anion/cation-π interactions, as shown in Fig. 3e.[23,35] As shown in Fig. 3f, the hydrogel can be easily bonded to and peeled off from human skin without leaving any residue on the skin's surface. Nanocomposite hydrogels based on abundant zwitterionic groups exhibit unparalleled adhesion ability for various substrates, which is of great importance for the application of wearable sensors.

3.6 Electromechanical properties

Due to the stretchability and strain-induced resistance change of the PSBMA-BCN hydrogel, it could potentially be applied as a resistivity-type sensor; the electromechanical properties under stretching deformation are presented in Fig. 4. The electromechanical properties of the PSBMA-BCN hydrogel sensors were determined by assembling the hydrogel into the structure shown in Fig. 4a. The gauge factor (GF) defines the sensitivity of the strain sensor, which is critical for its performance. To quantitatively evaluate the GF of the hydrogel sensor, a tensile measuring instrument was used in combination with a resistance measuring instrument. As shown in Fig. 4b, the hydrogel sensor exhibited excellent

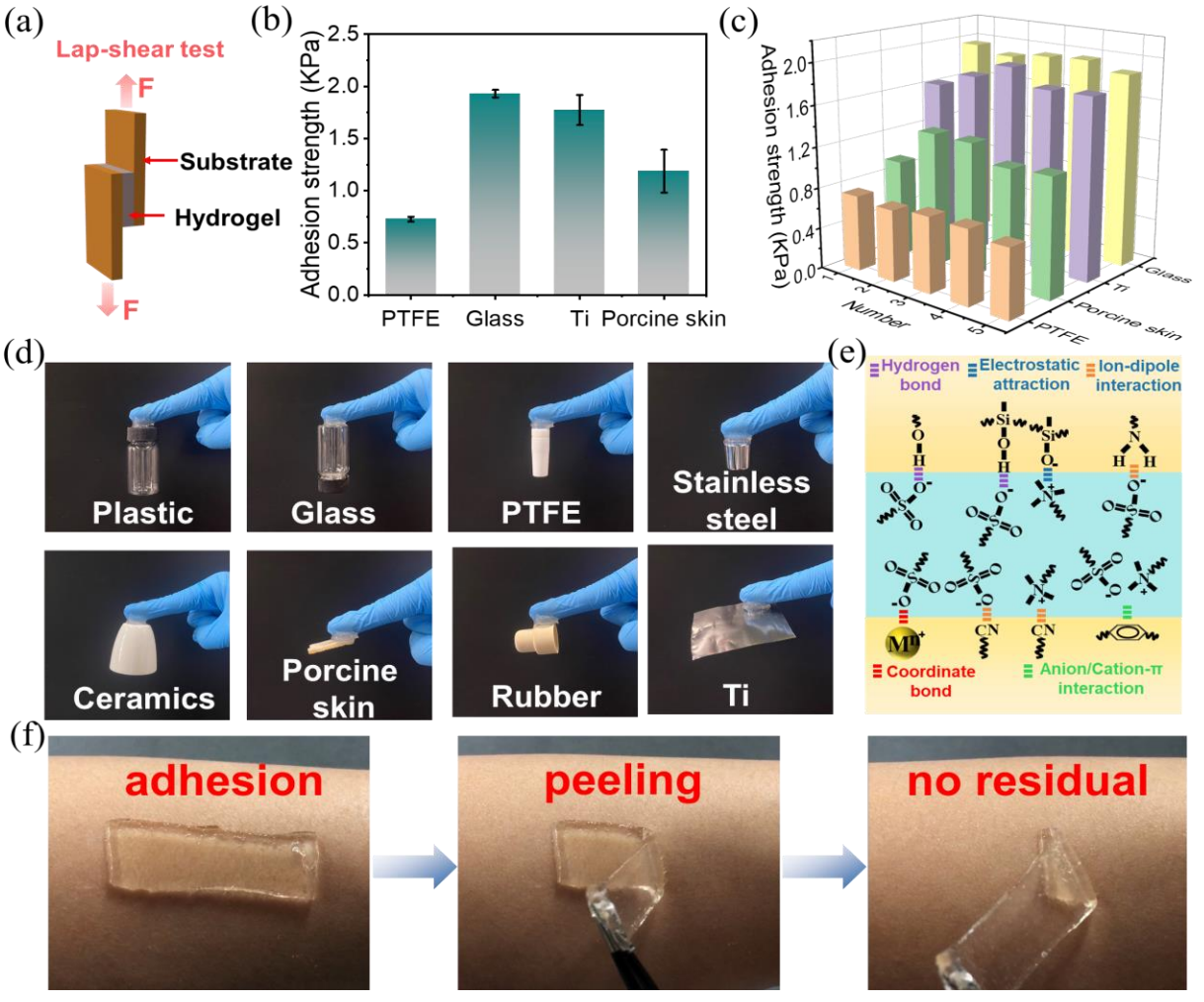

Fig. 3 Self-adhesive performance of hydrogels. (a) Schematic representation of the lap-shear test for the PSBMA-BCN hydrogel. (b) Adhesion strength of hydrogels on different substrates. (c) Repeatable adhesion strength of the hydrogel on different substrates. (d) Adhesion demonstrations. (e) Possible mechanisms of adhesion behavior. (f) Digital images of adhesive performance on human skin.

sensitivity even under small strains. The strain sensing performance of the hydrogels exhibited three linear regions. The calculated GF values were 1.6 within 50% strain, 1.9 within 50%-100%, and 2.2 within 100-180% strain, respectively. The PSBMA-BCN hydrogel sensor demonstrated a short response time (300 ms) and recovery time (300 ms) when subjected to loading and unloading with strain (Fig. 4c). Due to its fast electromechanical response, the hydrogel sensor exhibited nearly negligible electrical signal hysteresis under 10% strain (Fig. 4d). Additionally, the resistance change ratios (RRCs) of the hydrogel sensor under small strains (0.2%, 0.5%, 1%, and 5%) and large strains (10%, 50%, and 100%) were recorded, as depicted in Fig. 4e and Fig. S6. A clear difference in RRCs can be observed for both small and large strains. Notably, the hydrogel sensor can accurately and continuously monitor fine strains as low as 0.2%, with distinguishable and symmetrical RRCs, which play a key role in ultrasensitive wearable sensors. The frequency responsiveness, a vital parameter for wearable sensors, was also evaluated, as shown in Fig. 4f. The strain sensors maintained stable and rapid electromechanical responsiveness even at an applied test frequency of 5 Hz. More importantly, the strain sensors demonstrated long-term reliability and stability, evidenced by over ~100 cycles of dynamic stretching and releasing between 0 and 10% strain (Fig. 4g). These results demonstrate that the PSBMA-BCN hydrogel sensor can monitor different strains and generate targeted feedback electrical signals in real time. Furthermore, after soaking in water for 7 days, the sensing sensitivity, including the GF of the hydrogel sensor, was hardly affected (Fig. 4h). Additionally, the hydrogel sensor, after soaking in water, exhibited excellent reliability (Fig. 4i). These results indicate that the PSBMA-BCN hydrogel sensor can be effectively applied in aqueous environments. Given its outstanding sensing sensitivity, the PSBMA-BCN hydrogel sensor is an excellent candidate material for monitoring human movement

(Fig. S7).

3.7 Underwater application

With the rapid development of technology, an increasing number of human underwater activities will gradually be involved. To ensure the safety of underwater activities, it is worthwhile to research flexible electronic devices with underwater communication capabilities. As is well known, Morse code, which was developed for various types of information transmission, has been used for more than a century. It consists of "dots" and "dashes," and different arrangements can represent various letters of the Latin alphabet (Fig. 5a).

In this work, the PSBMA-BCN hydrogel demonstrated excellent anti-swelling performance, which not only endowed the hydrogel sensor with potential applications for communication in aquatic environments using Morse code but also enabled the detection of different bending angles of fingers underwater (Fig. 5b), thus providing possibilities for underwater communication through the PSBMA-BCN hydrogel sensor. To achieve information transfer, the sensor fabricated from the PSBMA-BCN hydrogel needs to be attached to a finger, and a new rule was established by combining Morse code with finger bending status. A small bending angle of less than 60° represents the "dots," while a large bending angle of around 90° represents the "dashes" (Fig. 5a). Based on this principle, a series of useful information can be easily transmitted in aquatic environments. During underwater activities, such as diving sports, the user wearing the hydrogel sensor can easily and quickly send brief messages by regularly bending their fingers in case of danger, such as sending an "SOS" for help (Fig. 5c). Additionally, the hydrogel sensor was capable of transmitting simple messages, such as "I am fine" (Fig. 5d). Furthermore, the hydrogel sensor can also transmit various types of information underwater, such as "Help," "OK," "Come here," and "Hurry up" (Fig. S8).

Based on the underwater communication capabilities of the hydrogel sensor, we designed a circuit and demonstrated the feasibility of wireless intelligent communication for the first time through computer programming. The wireless

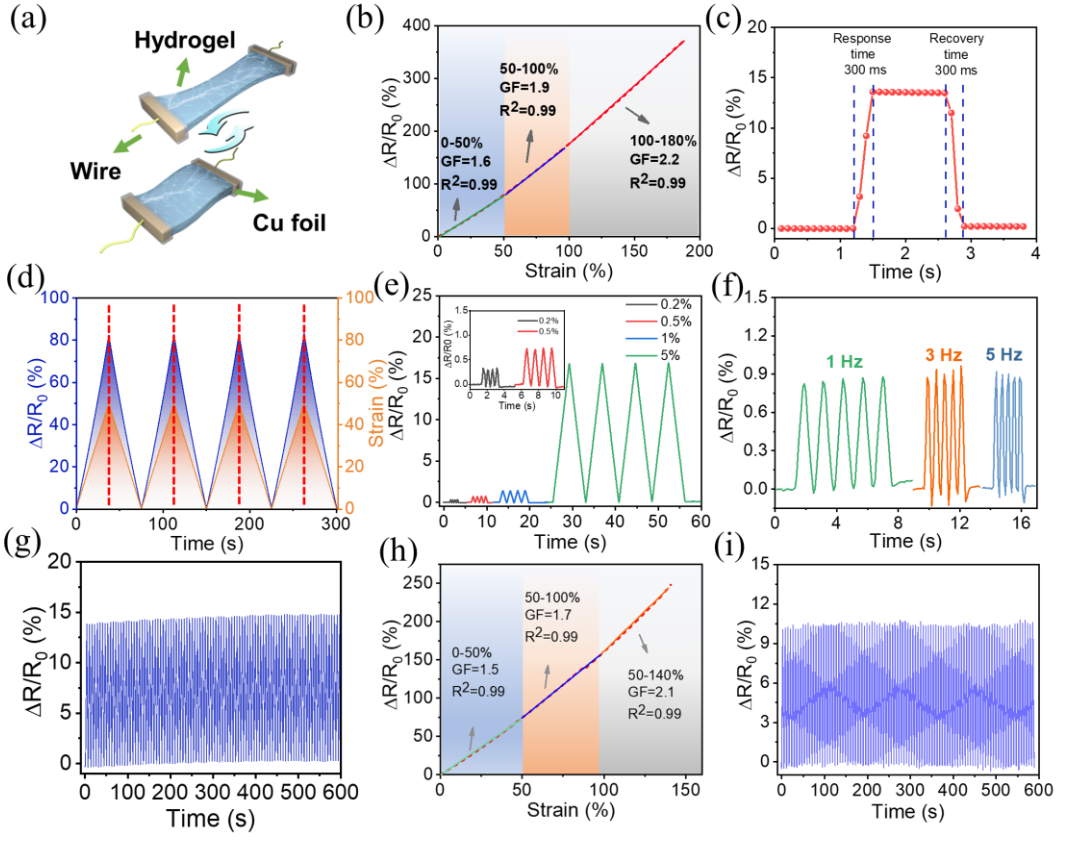

Fig. 4 Sensing properties of PSBMA-BCN hydrogel sensor. (a) Schematic diagram of the hydrogel sensor before and after stretching. (b) RRCs as a function of the applied strain. (c) Response time of hydrogel sensors when stretching under 10%. (d) Tensile strain–time curve and the relative resistance–time curve. (e) RRCs as a function of time applied different strain. (f) RRCs as a function of time applied different test frequency. (g) RRCs under repeated stretching/releasing cycles under strains of 10%. (h) RRCs of PSBMA-BC hydrogels as a function of applied strain after soaking in water for 7 days. (i) RRCs under repeated stretching/releasing cycles under strains of 10% after soaking in water for 7 days.

intelligent communication system not only facilitates the wireless transmission of signals but also intelligently converts regular electrical signals into text information, significantly enhancing the performance of underwater communication. As illustrated in Figs. S9a-b, the intelligent communication system includes a Bluetooth transmission module, a hydrogel sensor module, a microcontroller, and a current detection module. When the hydrogel sensor is attached to the finger, the principle of Morse code is employed, allowing the finger to bend regularly to convey signals. As complex information such as "Come here" and "I am fine" can be transmitted through the regular bending of fingers. These examples demonstrate that the PSBMA-BCN hydrogel sensor has potential applications as underwater communication equipment for activities such as underwater exploration, underwater sports, and underwater rescue.

In addition to being attached to a finger for communication, the hydrogel sensor can function as a flexible electronic device for motion detection. For instance, this hydrogel sensor can monitor fish movement in real time, benefiting fish kinematics research and providing guidance for fish farming. As a demonstration, the tail of an electric toy fish, used as a research object to simulate underwater motion, was equipped with the PSBMA-BCN hydrogel sensor to monitor its movements in water. As shown in Fig. 5g, during the swimming process, the electrical signal generated by tail movement can be continuously captured. Interestingly, the various swimming modes, including going straight, turning left, and turning right, can be determined by analyzing the shape of the electrical signal peaks. Specifically, as the fish

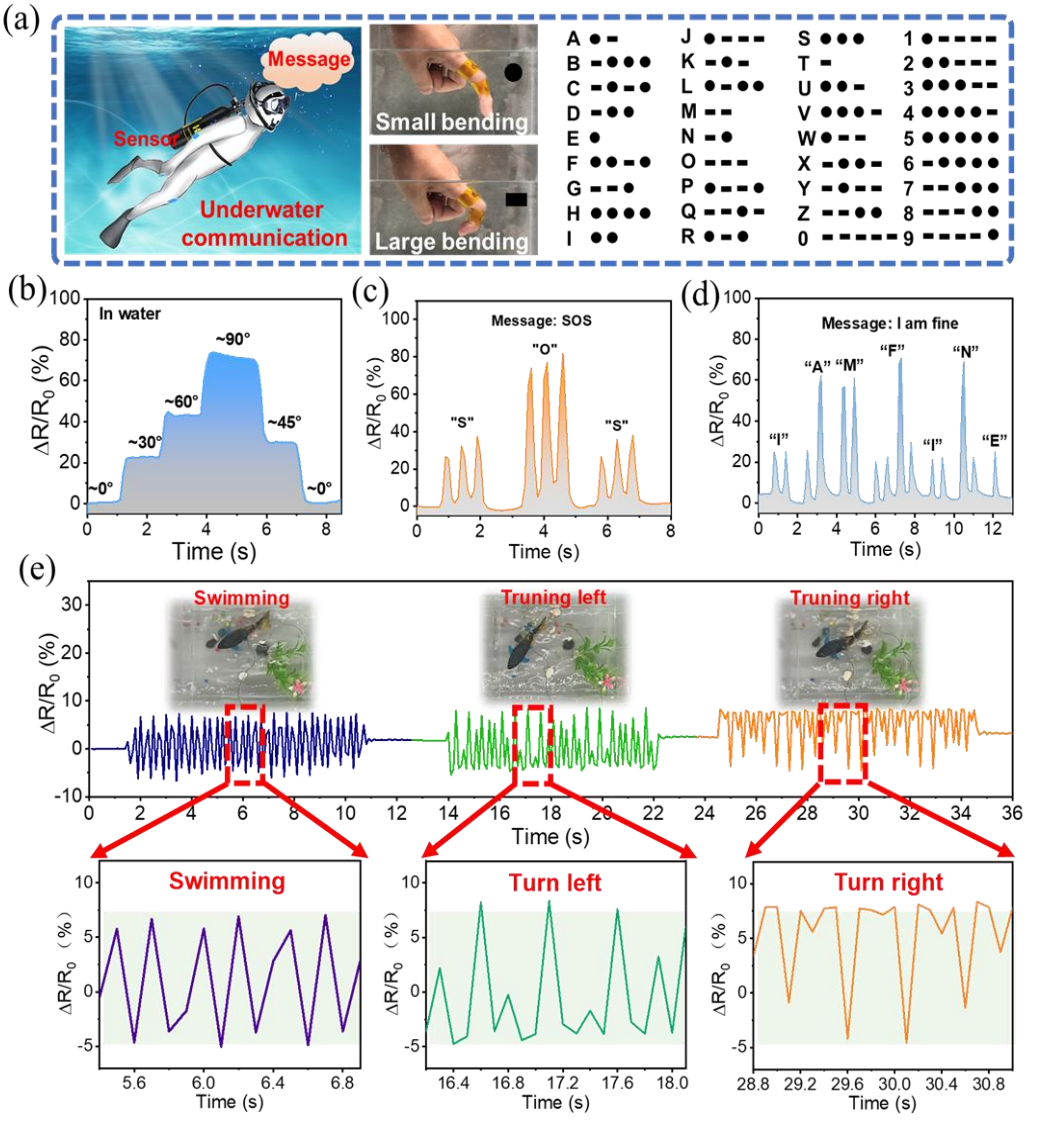

Fig. 5 Underwater applications utilizing the hydrogel sensor. (a) Schematic diagram of the hydrogel sensor attached to the finger for information transmission using Morse code. (b) RRCs of finger bending at various angles (30°, 45°, 60°, and 90°) in water. (c) and (d) Underwater communication using the hydrogel sensor through Morse code. (e) Real-time sensing signals from the hydrogel sensor monitoring the states of the fish model, including swimming, turning left, and turning right.

moves forward, left, or right, the flexible sensor attached to the tail is compressed or stretched to varying degrees at the same frequency, causing the captured electrical signal peaks to be symmetrical to the X-axis or deviate in the Y-axis or negative direction. Therefore, the movement mode of the fish in water can be easily identified. The experimental results demonstrated that the PSBMA-BCN hydrogel sensor can reliably and continuously monitor motions.

3.8 Biocompatible properties

For wearable electronic devices, particularly those in direct contact with the skin, biocompatibility is a crucial requirement, as it can prevent allergic reactions and protect the wearer from exposure to toxic substances. Additionally, considering the application environment, particularly liquid environments, biocompatible wearable sensors can mitigate toxic hazards in these settings. To assess the biocompatibility of the PSBMA-BCN hydrogel-based sensors, cell Live/Dead staining analysis was conducted (Fig. 6a). After 24 hours of culture with different extracts of the hydrogel, a small number of living cells (green fluorescent-labeled cells) were observed. After 48 hours, the number of living cells significantly increased, and almost no dead cells were observed (red fluorescence was not detected). Compared to the blank control group, there was no significant difference in cell number or viability among the experimental groups. Additionally, cytocompatibility was assessed by culturing human amniotic epithelial cells (HAECs) for 24 and 48 hours, respectively. Cell viability was evaluated using the Cell Counting Kit-8 (CCK-8) assay. As shown in Figs. 6b-c, the relative cell viability after 24 and 48 hours in all PSBMA-BCN hydrogel extracts exceeded 90%, indicating that the hydrogel did not affect cellular viability. These results demonstrated that the PSBMA-BCN hydrogel exhibited outstanding biocompatibility. Furthermore, skin compatibility was assessed by attaching the PSBMA-BCN hydrogel to a volunteer's arm, as shown in Fig. 6d. After 12 hours, the PSBMA-BCN hydrogel did not cause any allergic reactions, and no obvious inflammation was observed on the human skin.

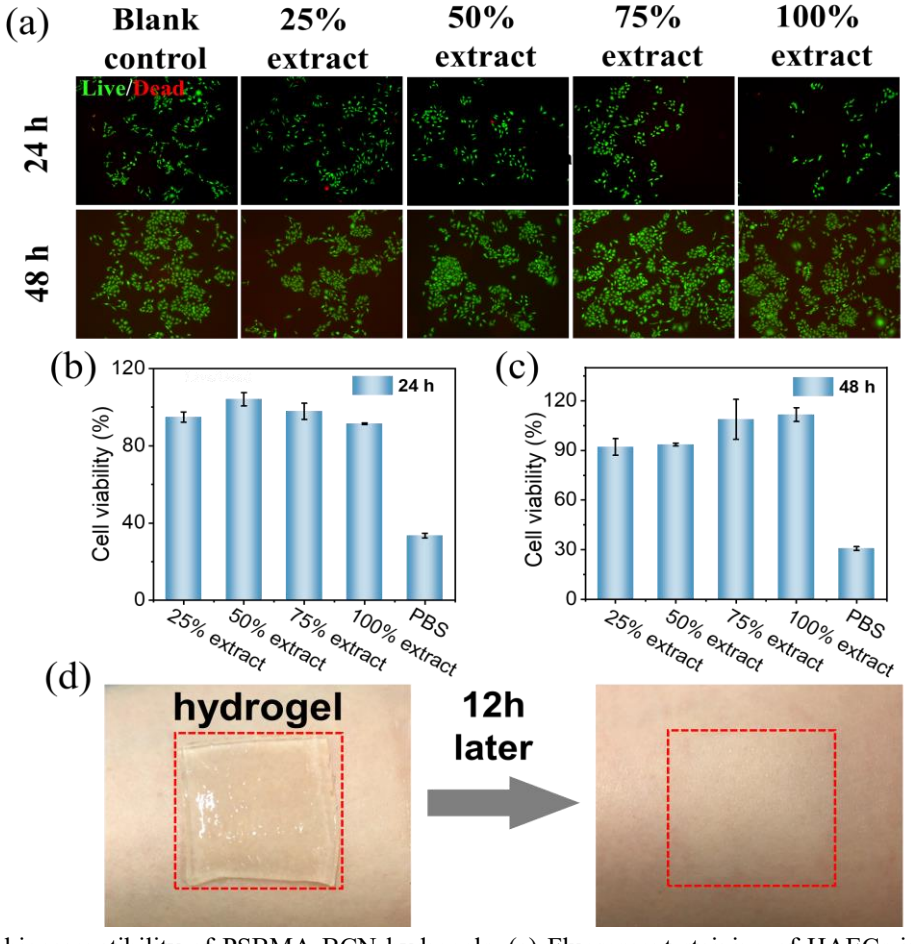

Fig. 6 Evaluation of the biocompatibility of PSBMA-BCN hydrogels. (a) Fluorescent staining of HAECs incubated in different hydrogel extracts for 2 days (blank control group: pure medium). Cell viability in PSBMA-BCN hydrogel extracts and the positive control group after (c) 24 hours and (d) 48 hours. (d) Photographs of the PSBMA-BCN hydrogels attached to the arm skin after 12 hours.

These results indicated that the PSBMA-BCN hydrogel exhibited excellent biocompatibility and is a promising candidate for wearable strain sensors intended for direct contact with the skin, particularly in underwater environments. Prior to conducting the skin compatibility experiment, the volunteer was informed about the details of the human study and agreed to participate.

4. Conclusions

In summary, we present an anti-swelling, biocompatible, and adhesive hydrogel wearable sensor developed from a composite of bacterial cellulose nanofibers and PSBMA. Specifically, the abundant zwitterionic functional groups, including negatively charged ($-SO_3^-$) and positively charged ($-R_3N^+$), enable the hydrogel to adhere to various substrates. Furthermore, the strong electrostatic interaction between $-SO_3^-$ and $-R_3N^+$ imparts the hydrogel with anti-swelling capacity. After soaking for 7 days in water and an acidic aqueous solution (pH = 3), the swelling ratios of the hydrogel were -11% and -10%, respectively. Notably, the mechanical and adhesion properties of the hydrogel were minimally affected. As a wearable sensor, it exhibited excellent sensing sensitivity with gauge factors of 1.6, 1.9, and 2.2 within the strain ranges of 0-50%, 50-100%, and 100-180%, respectively. After 700 cycles at 40% strain, the hydrogel sensor showed no signs of attenuation. Moreover, the hydrogel sensor can precisely respond to target movements and output signals in real time, enabling it to monitor and identify different movements effectively. More significantly, as a wearable electronic device designed for liquid environments, the hydrogel sensor can not only facilitate real-time monitoring and identification of target movements, but also enable intelligent underwater communication through the integration of computer programming and circuit design. Thus, as a promising candidate for underwater applications, the anti-swelling, biocompatible, and adhesive hydrogel sensor offers an effective approach for the next generation of intelligent wearable devices for underwater use.

Acknowledgements

We are grateful for Ms. Chunyan Zhong, Hainan Guangyu Biotechnology Co., Ltd. for kindly offer the BC samples. This work was supported by the National Natural Science Foundation of China (grant No. 21875068) and Fundamental Research Funds for the Central Universities (2020ECNU-GXJC003).

Conflict of Interest

There is no conflict of interest.

Supporting Information

Applicable.

References

[1] G. Ge, Y. Lu, X. Qu, W. Zhao, Y. Ren, W. Wang, Q. Wang, W. Huang, X. Dong, Muscle-inspired self-healing hydrogels for strain and temperature sensor, *ACS Nano*, 2020, **14**, 218-228, doi: 10.1021/acsnano.9b07874.

[2] J. Liu, H. Wang, R. Ou, X. Yi, T. Liu, Z. Liu, Q. Wang, Anti-bacterial silk-based hydrogels for multifunctional electrical skin with mechanical-thermal dual sensitive integration, *Chemical Engineering Journal*, 2021, **426**, 130722, doi: 10.1016/j.cej.2021.130722.

[3] Z. Jiang, Y. Wang, Z. Huang, W. Ma, S. Gao, W. Dong, M. Xu, Green and sustainable cellulose-based shape memory composites with excellent conductivity for temperature warning, *Carbohydrate Polymers*, 2022, **276**, 118767, doi: 10.1016/j.carbpol.2021.118767.

[4] H. Ding, Z. Xin, Y. Yang, Y. Luo, K. Xia, B. Wang, Y. Sun, J. Wang, Y. Zhang, H. Wu, S. Fan, L. Zhang, K. Liu, Ultrasensitive, low-voltage operational, and asymmetric ionic sensing hydrogel for multipurpose applications, *Advanced Functional Materials*, 2020, **30**, 1909616, doi: 10.1002/adfm.201909616.

[5] J. Huang, J. Zeng, X. Zhang, G. Guo, R. Liu, Z. Yan, Y. Yin, Fatigue resistant aerogel/hydrogel nanostructured hybrid for highly sensitive and ultrabroad pressure sensing, *Small*, 2022, **18**, 2104706, doi: 10.1002/smll.202104706.

[6] F. Mo, Y. Huang, Q. Li, Z. Wang, R. Jiang, W. Gai, C. Zhi, A highly stable and durable capacitive strain sensor based on dynamically super-tough hydro/organo-gels, *Advanced Functional Materials*, 2021, **31**, 2010830, doi: 10.1002/adfm.202010830.

[7] M. Ju, B. Wu, S. Sun, P. Wu, Redox-active iron-citrate complex regulated robust coating-free hydrogel microfiber net with high environmental tolerance and sensitivity, *Advanced Functional Materials*, 2020, **30**, 1910387, doi: 10.1002/adfm.201910387.

[8] T. Li, L. Li, H. Sun, Y. Xu, X. Wang, H. Luo, Z. Liu, T. Zhang, Humidity sensors: porous ionic membrane based flexible humidity sensor and its multifunctional applications, *Advanced Science*, 2017, **4**, 1600404, doi: 10.1002/advs.201770026.

[9] S. Choi, H. Lee, R. Ghaffari, T. Hyeon, D.-H. Kim, Recent advances in flexible and stretchable bio-electronic devices integrated with nanomaterials, *Advanced Materials*, 2016, **28**, 4203-4218, doi: 10.1002/adma.201504150.

[10] Q. Pang, D. Lou, S. Li, G. Wang, B. Qiao, S. Dong, L. Ma, C. Gao, Z. Wu, Smart flexible electronics-integrated wound dressing for real-time monitoring and on-demand treatment of infected wounds, *Advanced Science*, 2020, **7**, 1902673, doi: 10.1002/advs.201902673.

[11] W.-D. Li, K. Ke, J. Jia, J.-H. Pu, X. Zhao, R.-Y. Bao, Z.-Y. Liu, L. Bai, K. Zhang, M.-B. Yang, W. Yang, Recent advances in multiresponsive flexible sensors towards E-skin: a delicate design for versatile sensing, *Small*, 2022, **18**, 2103734, doi:

10.1002/smll.202103734.
[12] M. Wang, Y. Luo, T. Wang, C. Wan, L. Pan, S. Pan, K. He, A. Neo, X. Chen, Artificial skin perception, *Advanced Materials*, 2021, **33**, 2003014, doi: 10.1002/adma.202003014.
[13] T. Li, Y. Li, T. Zhang, Materials, structures, and functions for flexible and stretchable biomimetic sensors, *Accounts of Chemical Research*, 2019, **52**, 288-296, doi: 10.1021/acs.accounts.8b00497.
[14] G. Shi, Z. Zhao, J.-H. Pai, I. Lee, L. Zhang, C. Stevenson, K. Ishara, R. Zhang, H. Zhu, J. Ma, Highly sensitive, wearable, durable strain sensors and stretchable conductors using graphene/silicon rubber composites, *Advanced Functional Materials*, 2016, **26**, 7614-7625, doi: 10.1002/adfm.201602619.
[15] H.-R. Lee, C.-C. Kim, J.-Y. Sun, Stretchable ionics–A promising candidate for upcoming wearable devices, *Advanced Materials*, 2018, **30**, 1704403, doi: 10.1002/adma.201704403.
[16] H. Yuk, B. Lu, X. Zhao, Hydrogel bioelectronics, *Chemical Society Reviews*, 2019, **48**, 1642-1667, doi: 10.1039/c8cs00595h.
[17] L. Xu, S. Gao, Q. Guo, C. Wang, Y. Qiao, D. Qiu, A solvent-exchange strategy to regulate noncovalent interactions for strong and antiswelling hydrogels, *Advanced Materials*, 2020, **32**, 2004579, doi: 10.1002/adma.202004579.
[18] X. Liu, Q. Zhang, G. Gao, Solvent-resistant and nonswellable hydrogel conductor toward mechanical perception in diverse liquid media, *ACS Nano*, 2020, **14**, 13709-13717, doi: 10.1021/acsnano.0c05932.
[19] J. Liu, Z. Chen, Y. Chen, H. U. Rehman, Y. Guo, H. Li, H. Liu, Ionic conductive organohydrogels with dynamic pattern behavior and multi-environmental stability, *Advanced Functional Materials*, 2021, **31**, 2101464, doi: 10.1002/adfm.202101464.
[20] J. Wei, Y. Zheng, T. Chen, A fully hydrophobic ionogel enables highly efficient wearable underwater sensors and communicators, *Materials Horizons*, 2021, **8**, 2761-2770, doi: 10.1039/d1mh00998b.
[21] J. Ren, Y. Liu, Z. Wang, S. Chen, Y. Ma, H. Wei, S. Lü, An anti-swellable hydrogel strain sensor for underwater motion detection, *Advanced Functional Materials*, 2022, **32**, 2107404, doi: 10.1002/adfm.202107404.
[22] Z. Xu, C. Fan, Q. Zhang, Y. Liu, C. Cui, B. Liu, T. Wu, X. Zhang, W. Liu, A self-thickening and self-strengthening strategy for 3D printing high-strength and antiswelling supramolecular polymer hydrogels as meniscus substitutes, *Advanced Functional Materials*, 2021, **31**, 2100462, doi: 10.1002/adfm.202100462.
[23] Q. Fu, S. Hao, L. Meng, F. Xu, J. Yang, Engineering self-adhesive polyzwitterionic hydrogel electrolytes for flexible zinc-ion hybrid capacitors with superior low-temperature adaptability, *ACS Nano*, 2021, **15**, 18469-18482, doi: 10.1021/acsnano.1c08193.
[24] J. Yang, Z. Xu, J. Wang, L. Gai, X. Ji, H. Jiang, L. Liu, Antifreezing zwitterionic hydrogel electrolyte with high conductivity of 12.6 mS Cm−1 at −40 °C through hydrated lithium ion hopping migration, *Advanced Functional Materials*, 2021, **31**, 2009438, doi: 10.1002/adfm.202009438.
[25] J. Ding, H. Liang, X. Zhu, D. Xu, X. Luo, Z. Wang, L. Bai, Surface modification of nanofiltration membranes with zwitterions to enhance antifouling properties during brackish water treatment: a new concept of a "buffer layer", *Journal of Membrane Science*, 2021, **637**, 119651, doi: 10.1016/j.memsci.2021.119651.
[26] Z. Zhu, Q. Gao, Z. Long, Q. Huo, Y. Ge, N. Vianney, N. A. Daliko, Y. Meng, J. Qu, H. Chen, B. Wang, Polydopamine/poly(sulfobetaine methacrylate) Co-deposition coatings triggered by $CuSO_4/H_2O_2$ on implants for improved surface hemocompatibility and antibacterial activity, *Bioactive Materials*, 2021, **6**, 2546-2556, doi: 10.1016/j.bioactmat.2021.01.025.
[27] J. B. Schlenoff, Zwitteration: coating surfaces with zwitterionic functionality to reduce nonspecific adsorption, *Langmuir*, 2014, **30**, 9625-9636, doi: 10.1021/la500057j.
[28] J. Huang, M. Zhao, Y. Cai, M. Zimniewska, D. Li, Q. Wei, A dual-mode wearable sensor based on bacterial cellulose reinforced hydrogels for highly sensitive strain/pressure sensing, *Advanced Electronic Materials*, 2020, **6**, 1900934, doi: 10.1002/aelm.201900934.
[29] X. Li, L. He, Y. Li, M. Chao, M. Li, P. Wan, L. Zhang, Healable, degradable, and conductive MXene nanocomposite hydrogel for multifunctional epidermal sensors, *ACS Nano*, 2021, **15**, 7765-7773, doi: 10.1021/acsnano.1c01751.
[30] J. Wu, C. He, H. He, C. Cheng, J. Zhu, Z. Xiao, H. Zhang, X. Li, J. Zheng, J. Xiao, Importance of zwitterionic incorporation into polymethacrylate-based hydrogels for simultaneously improving optical transparency, oxygen permeability, and antifouling properties, *Journal of Materials Chemistry B*, 2017, **5**, 4595-4606, doi: 10.1039/c7tb00757d.
[31] K. Leng, G. Li, J. Guo, X. Zhang, A. Wang, X. Liu, J. Luo, A safe polyzwitterionic hydrogel electrolyte for long-life quasi-solid state zinc metal batteries, *Advanced Functional Materials*, 2020, **30**, 2001317, doi: 10.1002/adfm.202001317.
[32] Y. Lu, Y. Yue, Q. Ding, C. Mei, X. Xu, Q. Wu, H. Xiao, J. Han, Self-Recovery, Fatigue-Resistant, and Multifunctional Sensor Assembled by a Nanocellulose/Carbon Nanotube Nano complex-Mediated Hydrogel, *ACS Applied Materials & Interfaces*, 2021, **13**, 50281-50297, doi: 10.1021/acsami.1c16828.
[33] S. Hirotsu, Static and time-dependent properties of polymer gels around the volume phase transition, *Phase Transitions*, 1994, **47**, 183-240, doi: 10.1080/01411599408200347.
[34] Y. Yu, H. Yuk, G. A. Parada, Y. Wu, X. Liu, C. S. Nabzdyk, K. Youcef-Toumi, J. Zang, X. Zhao, Multifunctional "hydrogel skins" on diverse polymers with arbitrary shapes, *Advanced Materials*, 2019, **31**, 1807101, doi: 10.1002/adma.201807101.
[35] B. Yang, W. Yuan, Highly stretchable, adhesive, and mechanical zwitterionic nanocomposite hydrogel biomimetic skin, *ACS Applied Materials & Interfaces*, 2019, **11**, 40620-40628, doi: 10.1021/acsami.9b14040.